Inorg. Chem. **2003**, *42*, 7052–7059

Crystal Structures and Magnetic Properties of Two Octacyanotungstate(IV) and (V)-Cobalt(II) Three-Dimensional Bimetallic Frameworks§

Juan Manuel Herrera,† Anne Bleuzen,† Yves Dromzée,† Miguel Julve,*,‡ Francesc Lloret,‡ and Michel Verdaguer*,†

Laboratoire de Chimie Inorganique et Matériaux Moléculaires, Université Pierre et Marie Curie, Unité CNRS 7071, F-75252 Paris Cedex 05, France, and Departament de Química Inorgànica/ Instituto de Ciencia Molecular, Facultat de Química de la Universitat de València, Dr. Moliner 50, 46100 Burjassot (València), Spain

Received February 19, 2003

The synthesis, X-ray structures, and magnetic behavior of two new, three-dimensional compounds $[W^{IV}\{(\mu\text{-}CN)_4\text{-}Co^{II}(H_2O)_2\}_2\cdot 4H_2O]_n$ (**1**) and $[\{W^{V}(CN)_2\}_2\{(\mu\text{-}CN)_4Co^{II}(H_2O)_2\}_3\cdot 4H_2O]_n$ (**2**) are presented. Compound **1** crystallizes in the tetragonal system, space group *I*4/*m* with cell constants $a = b = 11.710(3)$ Å, $c = 13.003(2)$ Å, and $Z = 4$, whereas **2** crystallizes in the orthorhombic system, space group *Cmca* with cell constants $a = 13.543(5)$ Å, $b = 16.054(6)$ Å, $c = 15.6301(9)$ Å, and $Z = 4$. The structure of **1** shows alternating eight-coordinated W(IV) and six-coordinated Co(II) ions bridged by single cyanides in a three-dimensional network. The geometry of each $[W^{IV}(CN)_8]^{4-}$ entity in **1** is close to a square antiprism. Its eight cyanide groups are coordinated to Co(II) ions which have two coordinated water molecules in *trans* position. The structure of **2** consists of alternating eight-coordinated W(V) and six-coordinated Co(II) ions linked by single cyanide bridges in a three-dimensional network. Each $[W^{V}(CN)_8]^{3-}$ unit shows a geometry close to a square antiprism. Only six of its eight cyanide groups are coordinated to Co(II) ions while the other two are terminal. The Co(II) ion in **2** has the same CoN_4O_2 environment as in **1**. The magnetic behavior of **1** is that of magnetically isolated high spin Co(II) ions ($S_{Co} = {}^3/_2$), bridged by the diamagnetic $[W^{IV}(CN)_8]^{3-}$ units ($S_{W(IV)} = 0$). The magnetic behavior of **2**, where the high spin Co(II) ions are bridged by the paramagnetic $[W^{V}(CN)_8]^{3-}$ units [$S_{W(V)} = {}^1/_2$], is that of ferromagnetically coupled Co(II) and W(V) giving rise to an ordered ferromagnetic phase below 18 K. The magnetic properties of **1** are used as a blank to extract the parameters that are useful to analyze the magnetic data of compound **2**.

Introduction

The interest in the synthesis and the study of the magnetic properties of new molecule-based magnetic materials is increasing.[1−7] Some important goals in this field are the synthesis of high-T_C magnetic materials[8,9] and of compounds whose magnetic properties are changed by external stimuli.[10] Remarkable examples obtained with hexacyanometalates as building blocks are the vanadium−chromium systems with T_C above room temperature[9] and the photomagnetic cobalt−iron Prussian blue analogues.[11,12]

* To whom correspondence should be addressed. E-mail: miv@ccr.jussieu.fr (M.V.). Phone: (int.-33)144273059 (M.V.). Fax: (int.-33)-144273841 (M.V.). E-mail: miguel.julve@uv.es (M.J.). Phone: (int.-34) 963864856 (M.J.). Fax: (int.-34) 963864322 (M.J.)

† Université Pierre et Marie Curie.

‡ Facultat de Química de la Universitat de València.

§ The authors would like to dedicate this paper to the memory of Yves Dromzée, smart crystallographer and friend, who recently passed away.

(1) Kahn, O. *Molecular Magnetism*; VCH: New York, 1993.
(2) Miller, J. S.; Epstein, A. J. *Angew. Chem., Int. Ed. Engl.* **1994**, *33*, 385.
(3) Gatteschi, D., et al. *Magnetic Molecular Materials*; Gratteschi, D., Kahn, O., Miller, J. S., Palacid, F., Eds.; Kluwer: Dordrecht, 1991.
(4) Tamaki, H. Zhong, Z. J.; Matsumoto, N.; Kida, S.; Koikawa, M.; Achiwa, N.; Hashimoto, Y.; Okawa, H. *J. Am. Chem. Soc.* **1992**, *114*, 6974.
(5) Mallah, T.; Thiebaut, S.; Verdaguer, M.; Veillet, P. *Science* **1993**, *262*, 1554.
(6) William, R. E.; Girolami, G. S. *Inorg. Chem.* **1994**, *33*, 5165.
(7) Ohkoshi, S.; Abe, Y.; Fujishima, A.; Hashimoto, K. *Phys. Rev. Lett.* **1999**, *82*, 1285.
(8) Miller, J. S.; Epstein, A. J. *Science* **1991**, *252*, 1415.
(9) Ferlay, S.; Mallah, T.; Ouahes, R.; Veillet, P.; Verdaguer, M. *Nature* **1995**, *378*, 701.
(10) (a) Decurtins, S.; Gütlich, P; Köhler, C. P.; Spiering, H.; Hauser, A. *Chem. Phys. Lett.* **1984,** *105*, 1. (b) Decurtins, S.; Gütlich, P.; Hasselbach, M. K.; Hauser, A.; Spiering, H. *Inorg. Chem.* **1985**, *24*, 2174.

10.1021/ic034188+ CCC: $25.00
Published on Web 10/03/2003

More recently, octacyanometalate complexes appeared as new precursors since they were expected to bring an enhanced exchange interaction in bimetallic compounds thanks to a larger extension of the 4d or 5d magnetic orbitals and different geometries depending on the packing and/or the oxidation state of the metal center.[13] The expected structural flexibility can be important in light-induced electron-transfer processes.[12] Octacyanometalates were recently used as precursors of systems with a high spin ground state,[14] three-dimensional networks with T_C values higher than those of the corresponding Prussian blue analogues,[15] and new photomagnetic molecule-based magnets.[16]

In this paper, we report the synthesis, crystal structure, and magnetic properties of two three-dimensional compounds $[W^{IV}\{(\mu\text{-}CN)_4Co^{II}(H_2O)_2\}_2\cdot 4H_2O]_n$ (**1**) and $[\{W^{V}(CN)_2\}_2\{(\mu\text{-}CN)_4Co^{II}(H_2O)_2\}_3\cdot 4H_2O]_n$ (**2**) where high spin Co(II) ions ($S_{Co} = {}^3/_2$) coexist with either diamagnetic W(IV) ($S_W = 0$) (**1**) or paramagnetic W(V) ($S_W = {}^1/_2$) (**2**).

Experimental Section

Materials. The precursors $K_4[W(CN)_8]\cdot 2H_2O$ and $Na_3[W(CN)_8]\cdot 3H_2O$ were prepared according to literature methods.[17] All other chemicals were purchased from commercial sources and used as received. Elemental analyses (C, N, H) were performed at the Microanalytical Service of the University Pierre et Marie Curie in Paris. The Co/W molar ratios for **1** (2:1) and **2** (3:2) were determined by electron probe X-ray microanalysis at the Servicio Interdepartamental of the University of Valencia.

Synthesis of the Compounds. $[W^{IV}\{(\mu\text{-}CN)_4Co^{II}(H_2O)_2\}_2\cdot 4H_2O]_n$(1). Compound **1** was prepared in the dark by slow diffusion of concentrated aqueous solutions of $K_4[W(CN)_8]\cdot 2H_2O$ (0.1 g, 0.17 mmol) and $Co(NO_3)_2\cdot 6H_2O$ (0.5 g, 1.7 mmol) and KNO_3 (0.5 g, 5 mmol) in an H-tube. After a few weeks, red polyhedral crystals of **1** were formed. Without KNO_3, no crystals are formed. The crystals were collected, washed with a small amount of distilled water and ethanol, and air-dried. Anal. Calcd for $C_8H_{16}Co_2N_8O_8W$ **(1)**: C, 14.69; H, 2.47; N, 17.13. Found: C, 14.42; H, 2.44; N, 16.60%.

$[\{W^{V}(CN)_2\}_2\{(\mu\text{-}CN)_4Co^{II}(H_2O)_2\}_3\cdot 4H_2O]_n$ (2). Compound **2** was prepared in the dark by slow diffusion of concentrated aqueous solutions of $Na_3[W(CN)_8]\cdot 3H_2O$ and $Co(NO_3)_2\cdot 6H_2O$ in an H-tube at 40 °C. Compound **2** separates as dark red platelike crystals after two months. They were collected and washed with small portions of water and dried on filter paper. The crystals of **2** used for physical measurements were covered with liquid paraffin in order to prevent dehydration. Anal. Calcd for $C_{16}H_{20}Co_3N_{16}O_{10}W_2$ **(2)**: C, 16.84; H, 1.77; N, 19.64. Found: C, 15.72; H, 1.75; N, 17.80%.

Table 1. Selected Experimental and Crystal Data for **1** and **2**

	1	**2**
formula	$C_8H_{16}N_8O_8Co_2W$	$C_{16}H_{20}N_{16}O_{10}Co_3W_2$
fw	653.95	1140.94
system	tetragonal	orthorhombic
space group	*I*4/*m*	*Cmca*
a (Å)	11.710(3)	13.543(5)
b (Å)	11.710(3)	16.054(6)
c (Å)	13.003(2)	15.631(9)
V (Å^3)	1783.1(6)	3398(3)
Z	4	4
d_{calcd} (g/cm^3)	2.38	2.23
T (K)	296(1)	296(1)
λ (Å)	0.71069	0.71069
μ(Mo Kα), (mm^{-1})	8.47	8.39
reflns collected	2462	2287
unique reflns	1120	2137
R_{int}	0.07	0.08
reflns with $I > 3\sigma(I)$	928	1711
R_w[a]	0.0281	0.0321
R[b]	0.0223	0.0328

[a] $R_w = [\sum w(|F_o| - |F_c|)^2/\sum w(|F_o|)^2]^{1/2}$. [b] $R = \sum(|F_o| - |F_c|)/\sum|F_o|$.

Crystallographic Data Collection and Structure Determination. The determination of the unit cell parameters and the collection of intensity data for **1** and **2** were made at 295 K on a Enraf Nonius CAD4 diffractometer using crystals of dimensions 0.2 × 0.4 × 0.6 mm^3 (**1**) and 0.4 × 0.4 × 0.4 mm^3 (**2**). The single crystal of **2** was embedded in a glue envelope in order to avoid dehydration. Of the 1120 (**1**) and 2137 (**2**) unique reflections, 928 for (**1**) and 1711 for (**2**) with $I > 3\sigma(I)$ were used to solve the structure with SHELXS-86 program.[18] Computations were performed by using PC versions of CRYSTALS.[19] Least-squares refinements of 70 (for **1**) and 116 (for **2**) parameters with approximation to the normal matrix were carried out by minimizing the function $\sum w(|F_o| - |F_c|)^2$, where F_o and F_c are the observed and calculated structure factors. Corrections were made for Lorentz and polarization effects. Empirical absorption correction based on Ψ scan curves were applied. The models reached convergence with $R = 0.0223$ and $R_w = 0.0281$ for **1** and $R = 0.0328$ and $R_w = 0.0321$ for **2**. The hydrogen atoms were not included in the refinement. All non-hydrogen atoms were refined anisotropically. The crystallographic data for **1** and **2** are summarized in Table 1. Main bond lengths and angles are listed in Tables 2 (**1**) and 3 (**2**).

Physical Techniques. Infrared spectra of **1** and **2** were performed on a Bio-Rad FT-IR spectrometer FTS 165 on KBr pellets. Reflectance electronic spectra of **1** and the precursor $K_4[W(CN)_8]\cdot 2H_2O$ were performed in a Cary 5E (Varian) spectrometer in the solid phase between 6250 and 22000 cm^{-1}. Variable-temperature magnetic susceptibility data of polycrystalline samples of **1** and **2** were collected with a MPMS Quantum Design SQUID magnetometer (XL5S) in the 2.0−300 K temperature range under applied fields of 100 Oe (300−2.0 K) for **1** and 50 Oe (50−2.0 K) and 500 Oe (300−50 K) for **2**. Diamagnetic corrections[20] per $Co^{II}_2W^{IV}$

(11) (a) Sato, O.; Iyoda, T.; Fujishima, A.; Hashimoto, K. *Science* **1996**, *272*, 704−705. (b) Verdaguer, M. *Science* **1996**, *272*, 698.

(12) (a) Bleuzen, A.; Lomenech, C.; Escax, V.; Villain, F.; Varret, F.; Cartier dit Moulin, C.; Verdaguer, M. *J. Am. Chem. Soc.* **2000**, *122*, 6647 (b) Cartier dit Moulin, C.; Villain, F.; Bleuzen, A.; Arrio, M. A.; Sainctavit, P.; Lomenech, C.; Escax, V.; Baudelet, F.; Dartyge, E.; Gallet, J. J.; Verdaguer, M. *J. Am. Chem. Soc.* **2000**, *122*, 6653.

(13) Leipold, J. G.; Basson, S. S.; Roodt, A. *Adv. Inorg. Chem.* **1993**, *40*, 241.

(14) (a) Zhong, Z. J.; Seino, H.; Mizobe, Y.; Masanobu, H.; Fujishima, A.; Ohkoschi, S.; Hashimoto, K. *J. Am. Chem. Soc.* **2000**, *122*, 2952. (b) Larionova, J.; Gross, M.; Pilkinton, M.; Andres, H.; Stoeckli-Evans, H.; Güdel, H. U.; Decurtins, S. *Angew. Chem., Int. Ed.* **2000**, *39*, 9, 1605.

(15) Zhong, Z. J.; Seino, H.; Mizobe, Y.; Hidai, M.; Verdaguer, M.; Ohkoshi, S.; Hashimoto, K. *Inorg. Chem.* **2000**, *39*, 5095.

(16) Ohkoschi, S.; Machida, N.; Zhong, Z. J.; Hashimoto, K. *Synth. Met.* **2001**, *122*, 523. (b) Rombaut, G.; Verelst, M.; Golhen, S.; Ouahab, L.; Mathonière, C.; Kahn, O. *Inorg. Chem.* **2001**, *40*, 1151. (c) Rombaut, G.; Golhen, S.; Ouahab, L.; Mathonière, C.; Kahn, O. *J. Chem. Soc., Dalton Trans.* **2000**, 3609.

(17) Leipoldt, J. G.; Bok, L. D. C.; Cilliers, P. J. *Z. Anorg. Allg. Chem.* **1974**, *407*, 350. (b) Baadsgaard, H.; Treadwell. *Helv. Chim. Acta*, **1955**, *201*, 1669.

(18) Sheldrick, G. M. *SHELXS 86, A program for crystal structure determination*; University of Göttingen: Göttingen, Germany, 1986.

(19) Watkin, D. J.; Carruthers, J. K.; Betteridge, P. W. *CRYSTALS, An advanced Crystallographic Program System*; Chemical Crystallography Laboratory: Oxford, U.K., 1989.

(20) Earnshaw, A. *Introduction to Magnetochemistry*; Academic Press: London and New York, 1968.

Table 2. Interatomic Distances (Å) and Bond Angles (deg) for Compound **1**[a]

W(1)−C(1)	2.162(3)	W(1)−C(2i)	2.158(3)
Co(1)−N(1)	2.099(3)	Co(1)−N(2)	2.134(3)
Co(1)−O(1)	2.085(5)	Co(1)−O(2)	2.116(4)
C(1)−N(1)	1.144(5)	C(2)−N(2)	1.150(5)
C(1)−W(1)−C(1ii)	72.6(9)	C(1)−W(1)−C(1iii)	113.7(2)
C(1)−W(1)−C(2i)	147.2(1)	C(1)−W(1)−C(2iv)	138.1(1)
C(1)−W(1)−C(2v)	76.0(1)	C(1)−W(1)−C(2vi)	81.7(1)
C(2i)−W(1)−C(2v)	113.5(2)	C(2i)−W(1)−C(2vi)	72.5(9)
N(1)−Co(1)−N(1vii)	89.6(2)	N(1)−Co(1)−N(2)	177.2(1)
N(1)−Co(1)−N(2vii)	92.5(1)	N(1)−Co(1)−O(1)	87.0(1)
N(1)−Co(1)−O(2)	90.9(1)	N(2)−Co(1)−N(2vii)	85.5(2)
N(2)−Co(1)−O(1)	95.1(1)	N(2)−Co(1)−O(2)	87.1(1)
O(1)−Co(1)−O(2)	177.0(2)		
W(1)−C(1)−N(1)	176.3(3)	W(1viii)−C(2)−N(2)	175.0(3)
Co(1)−N(1)−C(1)	166.5(3)	Co(1)−N(2)−C(2)	155.9(3)

[a] Symmetry codes: i = $^1/_2 + x$, $-^1/_2 + y$, $^1/_2 + z$; ii = $1 - y$, x, z; iii = $1 - x$, $1 - y$, z; iv = $-^1/_2 + y$, $^1/_2 - x$, $^1/_2 + z$; v = $^1/_2 - x$, $^3/_2 - y$, $^1/_2 + z$; vi = $^3/_2 - y$, $^1/_2 + x$, $^1/_2 + z$; vii = x, y, $1 - z$; viii = $-^1/_2 + x$, $^1/_2 + y$, $-^1/_2 + z$; ix = $1 - x$, $2 - y$, $1 - z$; x = y, $1 - x$, $1 - z$; xi = y, $1 - x$, z; xii = $-^1/_2 + y$, $^1/_2 - x$, $^3/_2 - z$; xiii = $^1/_2 - y$, $^1/_2 + x$, $^3/_2 - z$.

Table 3. Interatomic Distances (Å) and Bond Angles (deg) for Compound **2**

W(1)−C(1)	2.168(4)	W(1)−C(2)	2.143(5)
W(1)−C(3)	2.164(5)	W(1)−C(4)	2.159(4)
Co(1)−N(1)	2.117(4)	Co(1)−N(4i)	2.113(4)
Co(1)−O(1)	2.073(5)	Co(1)−O(2)	2.082(7)
Co(2)−N(2)	2.068(4)	Co(2)−O(3)	2.080(5)
C(1)−N(1)	1.138(6)	C(2)−N(2)	1.144(6)
C(3)−N(3)	1.132(7)	C(4)−N(4)	1.151(6)
C(1)−W(1)−C(1ii)	79.3(2)	C(1)−W(1)−C(2)	74.0(2)
C(1)−W(1)−C(2ii)	142.9(2)	C(1)−W(1)−C(3)	77.2(2)
C(1)−W(1)−C(3ii)	74.0(2)	C(1)−W(1)−C(4)	144.0(2)
C(1)−W(1)−C(4ii)	111.4(2)	C(2)−W(1)−C(2ii)	140.5(2)
C(2)−W(1)−C(3)	75.3(2)	C(2)−W(1)−C(3ii)	118.1(2)
C(2)−W(1)−C(4)	78.8(2)	C(2)−W(1)−C(4ii)	71.3(2)
C(3)−W(1)−C(3ii)	142.3(3)	C(3)−W(1)−C(4)	73.5(2)
C(3)−W(1)−C(4ii)	141.0(2)	C(4)−W(1)−C(4ii)	80.6(2)
N(1)−Co(1)−N(1iii)	89.1(2)	N(1)−Co(1)−N(4iv)	89.1(2)
N(1)−Co(1)−N(4i)	174.1(2)	N(1)−Co(1)−O(1)	92.9(1)
N(1)−Co(1)−O(2)	87.3(2)	N(4i)−Co(1)−N(4iv)	92.2(2)
N(4i)−Co(1)−O(1)	92.7(2)	N(4i)−Co(1)−O(2)	87.0(2)
O(1)−Co(1)−O(2)	179.6(2)	N(2)−Co(2)−N(2v)	180.
N(2)−Co(2)−N(2iii)	90.7(2)	N(2)−Co(2)−N(2vi)	89.3(2)
N(2)−Co(2)−O(3)	88.0(2)	N(2)−Co(2)−O(3v)	92.0(2)
O(3)−Co(2)−O(3v)	180.	W(1)−C(1)−N(1)	179.1(4)
W(1)−C(2)−N(2)	176.5(4)	W(1)−C(3)−N(3)	177.2(5)
W(1)−C(4)−N(4)	175.9(4)	Co(1)−N(1)−C(1)	165.2(4)
Co(2)−N(2)−C(2)	163.2(4)	Co(1vii)−N(4)−C(4)	163.1(4)

[a] Symmetry codes: i = $^1/_2 + x$, $-^1/_2 + y$, z; ii = $^1/_2 - x$, y, $^3/_2 - z$; iii = $1 - x$, y, z; iv = $^1/_2 - x$, $-^1/_2 + y$, z; v = $1 - x$, $1 - y$, $1 - z$; vi = x, $1 - y$, $1 - z$; vii = $-^1/_2 + x$, $^1/_2 + y$, z; viii = $^1/_2 - x$, $^1/_2 - y$, $1 - z$; ix = $^1/_2 + x$, $^1/_2 - y$, $1 - z$; x = x, $^1/_2 - y$, $^1/_2 + z$; xi = x, $^1/_2 - y$, $-^1/_2 + z$; xii = $1 - x$, $^1/_2 - y$, $-^1/_2 + z$.

(1) and $Co^{II}_3W^{V}_2$ **(2)** molar units were estimated as -243×10^{-6} **(1)** and -412×10^{-6} cm^3mol^{-1} **(2)**.

Results and Discussion

IR and Electronic Spectra. Compound **1** exhibits an intense cyanide stretching vibration band at 2134 cm^{-1} with a shoulder around 2151 cm^{-1} to be compared with the strong absorptions at 2130, 2125, and 2096 cm^{-1} in the IR spectrum of the ionic salt $K_4[W(CN)_8]\cdot 2H_2O$.[21] Such a shift of the ν_{CN} band toward higher frequencies in **1** is observed when the nitrogen of the cyanide is coordinated to another metal ion.[22] This shift and the absence of bands at lower frequencies in the cyanide stretching region suggest that all the cyanide groups are bridging.

The infrared spectrum of compound **2** shows three cyanide stretching vibration bands at 2201, 2178, and 2162 cm^{-1}. The band at 2162 cm^{-1} is also present in the IR spectrum of the ionic salt $Na_3[W(CN)_8]\cdot 3H_2O$, and it can be attributed to terminal cyanide groups. The other two peaks are shifted to higher frequencies compared to those of $Na_3[W(CN)_8]\cdot 3H_2O$, and they are associated with bridging cyanide groups. The bridging (**1** and **2**) and monodentate (**2**) coordination modes of the cyanide ligands suggested by the IR data are confirmed by the X-ray structures.

To obtain the electronic spectra of the high spin Co(II) ion unit $[Co(NC)_4(OH)_2]$ in **1**, we recorded the UV−vis spectra of **1** and of the precursor $K_4[W(CN)_8]\cdot 2H_2O$ (Figure S1) and got the difference spectrum, where two absorption peaks at 8784 cm^{-1} (ν_1) and 20575 cm^{-1} (ν_3) and a shoulder at 16639 cm^{-1} (ν_2) (Figure S2) are visible. The frequencies of the three spin-allowed transitions expected for a high spin Co(II) ion in a pseudo-octahedral geometry are related to the ligand field Dq and Racah B parameters through the eqs 1−3.[23]

$$\nu_1 = 5Dq - (^{15}/_2)B + {}^1/_2(225B^2 + 100Dq^2 + 180DqB)^{1/2} \quad (1)$$

$$\nu_2 = 15Dq - (^{15}/_2)B + {}^1/_2(225B^2 + 100Dq^2 + 180DqB)^{1/2} \quad (2)$$

$$\nu_3 = (225B^2 + 100Dq^2 + 180DqB)^{1/2} \quad (3)$$

These allow us to compute the values of $Dq = 786$ cm^{-1}, $B = 724$ cm^{-1}, and $Dq/B = 1.08$, relevant for the analysis of the magnetic behavior of compound **1** (see the following description).

Crystal Structure of $[W^{IV}\{(\mu\text{-}CN)_4Co^{II}(H_2O)_2\}_2\cdot 4H_2O]_n$ (1) and $[\{W^{V}(CN)_2\}_2\{(\mu\text{-}CN)_4Co^{II}(H_2O)_2\}_3\cdot 4H_2O]_n$ (2). Compound (**1**) crystallizes in the tetragonal system, space group $I4/m$. The structure is made up of a three-dimensional arrangement of W(IV) and Co(II) cations which alternate regularly and are bridged by single cyanide ligands. Hydrogen bonds involving the coordinated and crystallization water molecules (Table S1) contribute to the stabilization of the three-dimensional structure. A [001] projection of the crystal structure is shown in Figure 1a whereas a CAMERON representation of the tungsten and cobalt environments is shown in Figure 1b. The tungsten atom is coordinated by eight C-bonded cyanide ligands, and it exhibits a geometry close to a square antiprism. A crystallographic 4-fold rotation axis passes through the tungsten atom. The cobalt atom is six-coordinated with four N-bonded cyanides in equatorial positions and two oxygen atoms from two water molecules in axial positions of a distorted octahedron. A mirror plane contains the cobalt and the two oxygen atoms.

(21) Kettle, S. F. A.; Parish, R. V. *Spectrochim. Acta* **1965**, *21*, 1087.
(22) Nakamoto, K. *Infrared and Raman spectra of inorganic and coordination compounds*, 4th ed.; Wiley-Interscience: New York, 1986; p 272.
(23) Lever, A. B. P. *J. Chem. Educ.* **1968**, *11*, 711−712.

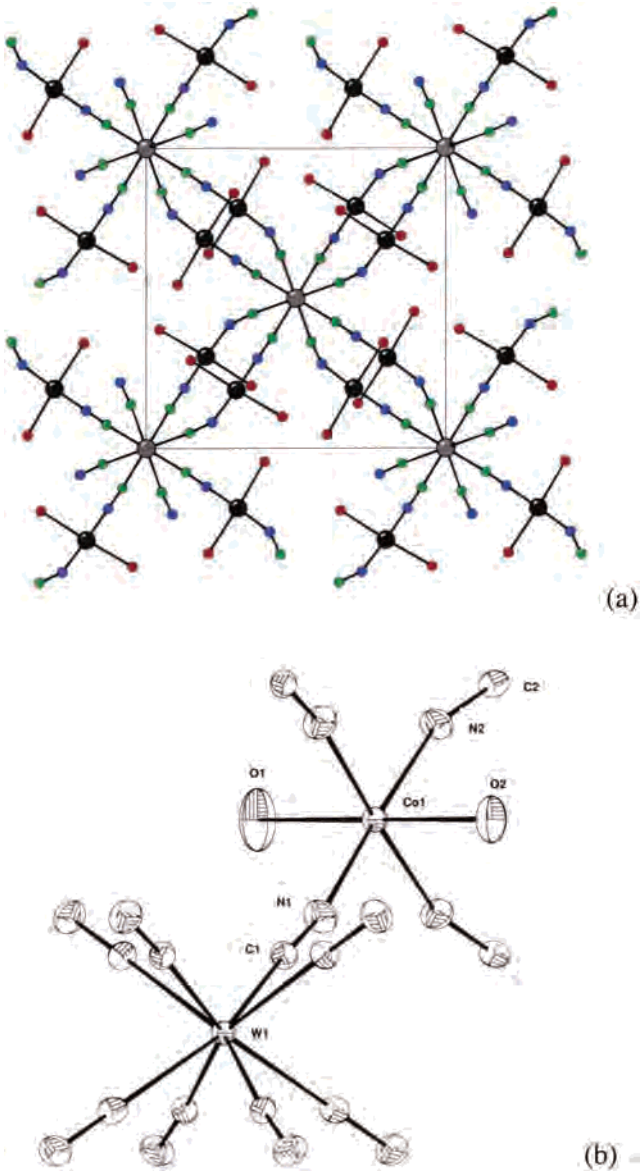

Figure 1. (a) [001] projection of the crystal structure of **1**. H atoms and crystallization water molecules are omitted for clarity (Co(1) black). (b) CAMERON representation of the W(IV) and the Co(II) coordination of **1**, with atomic numbering. H atoms are omitted. Thermal ellipsoids are drawn at the 50% probability level.

In **1**, the average values of the W−C (2.16 Å), C−N (1.15 Å), Co−N (2.12 Å), and Co−O (2.10 Å) bond distances are as observed in previously reported analogues.[24,25] The W−C1−N1 (176.3°) and W−C2−N2 (175.0°) angles are almost linear, while the Co−N1−C1 (166.5°) and Co−N2−C2 (155.9°) angles deviate strongly from linearity. The bond angles around the cobalt range from 87.5° to 95.1°. The shortest distance between the cyano-bridged W(IV) and the Co(II) ions is 5.405 Å. Three isostructural compounds of compound **1** based on $[M^{IV}(CN)_8]^{4-}$ (M = Nb, W, and Mo) and Mn^{II} ions will be reported elsewhere by some of us.[25]

(24) Rombaut, G.; Mathonière, C.; Guionneau, P.; Golhen, S.; Ouahab, L.; Verelsdt, M.; Lecante, P. *Inorg. Chim. Acta*, **2001**, *326*, 27.
(25) Franz, P.; Herrera, J. M.; Pilkington, M.; Biner, M.; Decurtins, S.; Stoeckli-Evans, H.; Neels, A.; Bleuzen, A.; Dromzee, Y.; Verdaguer, M.; Hashimoto, K. Manuscript in preparation.

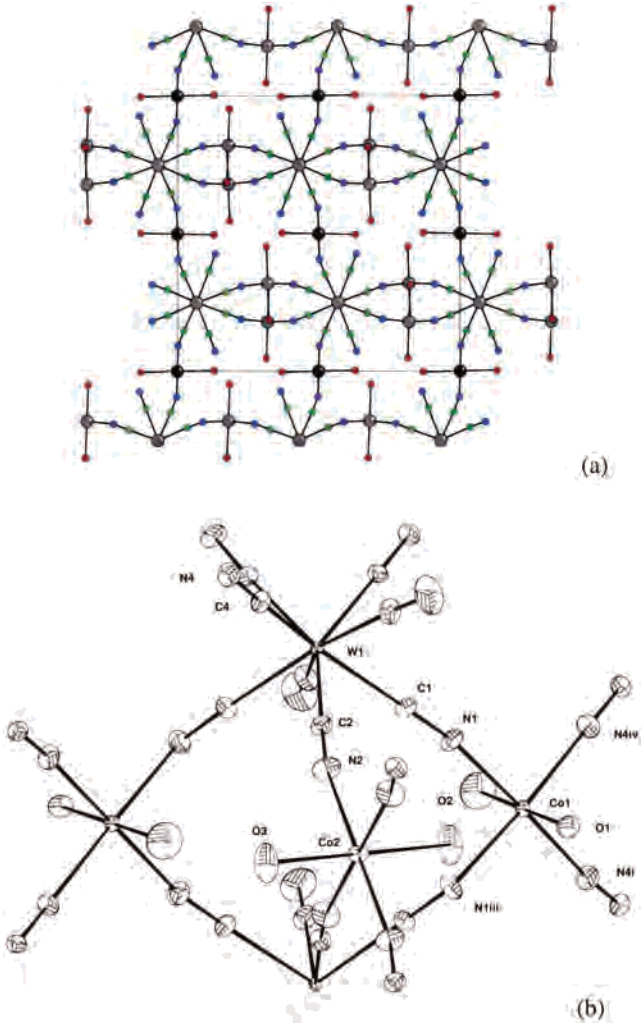

Figure 2. (a) [100] projection of the crystal structure of **2**. H atoms and crystallization water molecules are omitted. [Co(1) gray, Co(2) black]. (b) CAMERON representation of the W^V and the Co^{II} coordination of **2**, with atomic numbering. H atoms are omitted. Thermal ellipsoids are drawn at the 50% probability level.

Compound **2** consists of a three-dimensional bimetallic network $[\{W^V(CN)_2\}_2\{(\mu\text{-}CN)_4Co^{II}(H_2O)_2\}_3]_n$ and crystallization water molecules. Compound **2** crystallizes in the orthorhombic system, space group *Cmca*. A [100] projection of the crystal structure is shown in Figure 2a. A CAMERON representation of the W(V) and the Co(II) coordination with the atom numbering is shown in Figure 2b. The geometry around the $[W^V(CN)_8]$ entity is close to a square antiprism. Six cyanide ligands are linked to cobalt ions whereas the other two are terminal ones. There are two crystallographically independent cobalt atoms, Co(1) and Co(2). Both are in a distorted octahedral geometry, six-coordinated to four cyanide nitrogen atoms [N(1), N(1iii), N(4i), N(4iv) for Co(1) and N(2), N(2iii), N(2v), and N(2vi) for Co(2); symmetry codes: i = $^1/_2 + x$, $-^1/_2 + y$, z; iii = $1 - x$, y, z; iv = $^1/_2 - x$, $-^1/_2 + y$, z; v = $1 - x$, $1 - y$, $1 - z$; vi = x, $1 - y$, $1 - z$] and to two water molecules [O(1), O(2) for Co(1) and O(3), O(3v) for Co(2); symmetry codes: v = $1 - x$, $1 - y$, $1 - z$]. The four Co−N bond lengths are close to 2.115(4) Å around Co(1) and at 2.068(4) Å around Co(2), whereas the two Co−O distances are around 2.080-

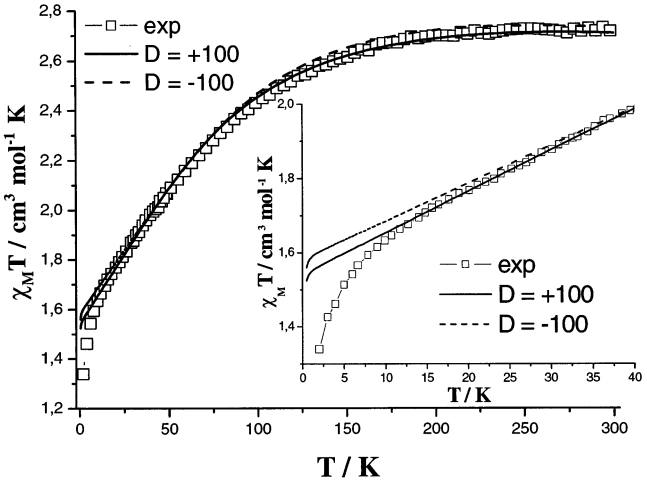

Figure 3. Thermal dependence of the $\chi_M T$ product for compound **1** per Co: (○) experimental; (— and - - -) best-fits through eq 6. The inset shows the low-temperature region.

(6) Å on both cobalt sites. The bond angles at the cobalt atoms range from 87.0(2)° to 92.9(1)° [Co(1)] and from 88.0(2)° to 92.0(2)° [Co(2)].

As in **1**, the W−C1−N1 (179.1°), W−C2−N2 (176.5°), W−C3−N3 (177.2°), and W−C4−N4 (175.9°) bond angles in **2** deviate slightly from linearity whereas Co1−N1−C1 (165.2°) and Co2−N2−C2 (163.2°) depart significantly from 180°.

Magnetic Properties of 1 and 2. The magnetic properties of complex **1** in the form of a $\chi_M T$ versus T plot (χ_M is the magnetic susceptibility per mol of Co(II)) are shown in Figure 3.

At room temperature, $\chi_M T$ is 2.72 cm^3 mol^{-1} K (μ_{eff} per Co(II) = 4.67 $N_A\beta$, N_A is the Avogadro constant and β the Bohr magneton), in agreement with one spin $S = {}^3/_2$ with unquenched angular momentum ($\mu_{eff(spin\ only,g=2)} = 3.87\ N_A\beta$). When lowering the temperature, $\chi_M T$ slowly decreases and reaches 1.34 cm^3 mol^{-1} K at 2.0 K. The decrease may be due to an antiferromagnetic exchange coupling between the Co(II) ions and/or to the depopulation of the higher energy Kramers doublets of the Co(II) centers.[26]

The cobalt−cobalt separation through the diamagnetic octacyanotungstate(IV) building units is more than 10.8 Å, and the exchange coupling between the $S = {}^3/_2$ centers is expected to be very weak. Consequently, the magnetic behavior of **1** can be assigned to magnetically isolated six-coordinated high spin Co(II) ions. The magnetic properties of **1** can be viewed as a model of the magnetic behavior of the Co(II) ions in **2**, since the environment of Co(II) is very similar in **1** and **2**.

Here, we describe the steps that we followed to check this hypothesis and to get a reasonable fit of the susceptibility data through the model of magnetically isolated high spin Co(II) ions in **1**.

The single-ion excited states for high spin Co(II) in O_h symmetry are well separated from the $^4T_{1g}$ ground state ($^4T_{1g} - {}^4T_{2g} = 8784$ cm^{-1} from the electronic spectrum). They are not thermally populated. The $^4T_{1g}$ ground state is split into a sextet, a quartet, and a Kramers doublet by spin−orbit coupling.[1,27] The corresponding Hamiltonian is

$$\mathbf{H}_{SO} = -Ak\lambda\mathbf{LS} \tag{4}$$

where k is the orbital reduction factor and λ is the spin−orbit coupling constant. The A factor, in the frame of T and P term isomorphism, allows us to distinguish between the matrix elements of the orbital angular momentum operator calculated with the wave functions of the ground $^4T_{1g}$ term with those calculated with the use of the P term basis ($|1, -1\rangle$, $|1, 0\rangle$ and $|1, -1\rangle$). A is defined by the equation $\mathbf{L}(T_{1g}) = -A\mathbf{L}(P)$ and can be written as eq 5:

$$A = \frac{{}^3/_2 - c^2}{1 + c^2} \tag{5}$$

The value c is the mixing coefficient of the $^4T_{1g}$ (F) and $^4T_{1g}$ (P) terms (eq 6):

$$\psi(^4T_{1g}) = \frac{1}{\sqrt{1 + c^2}}[\varphi^0(^4T_{1g}, F) + c\varphi^0(^4T_{1g}, P)] \tag{6}$$

The c value is calculated from Dq and B parameters through eq 7:

$$c = 0.75 + 1.875\frac{B}{Dq} - 1.25\left[1 + 1.8\frac{B}{Dq} + 2.25\left(\frac{B}{Dq}\right)^2\right]^{1/2} \tag{7}$$

Equation 5 describes the dependence of A on the strength of the crystal field Dq. In the weak crystal field limit ($B \gg Dq$), $c = 0$ and $A = {}^3/_2$, values used in most of the magnetic studies of Co(II) whereas in the strong crystal field limit ($B \ll Dq$), $c = -{}^1/_2$ and $A = 1$. In the present case, the electronic spectrum of **1** gives $B/Dq = 1.08$, $c = -0.175$, and $A = 1.425$.

In **1**, the six-coordinated Co(II) ion can be described as axially distorted (four cyanide-nitrogen atoms and two water molecules in *trans* positions), being approximately C_{4v}. Under an axial distortion, the triplet orbital $^4T_{1g}$ ground state splits into singlet $^4A_2$ and doublet ^4E levels with a D energy gap. The one-center operator responsible for an axial distortion is expressed by eq 8:

$$\mathbf{M}_{ax} = D\left[\mathbf{L}_z^2 - \frac{1}{3}L(L + 1)\right] \tag{8}$$

The Hamiltonian involving the spin−orbit coupling, axial distortion and Zeeman interaction is given by eq 9:

$$\mathbf{H} = -A\kappa\lambda\mathbf{LS} + D\left[\mathbf{L}_z^2 - \frac{1}{3}L(L + 1)\right] + \beta(-A\kappa\mathbf{L} + g_e\mathbf{S})H \tag{9}$$

No analytical expression for the magnetic susceptibility as a function of A, κ, λ, and D can be derived. The values of these parameters were determined through numerical matrix diagonalization. The best fit parameters of the experimental data for $T > 10$ K are $A = 1.423$ (i.e., $B/Dq = 1.05$ and c

(26) Banci, L.; Bencini, A.; Benelli, C.; Gatteschi, D.; Zanchini, C. *Struct. Bonding (Berlin)* **1982**, *52*, 37.

(27) Figgis, B. N.; Gerloch, M.; Lewis, J.; Mabbs, F. E.; Webb, G. A. *J. Chem. Soc. A* **1968**, 2086.

$= -0.177$), $k = 0.73$, $\lambda = -166$ cm^{-1}, and $D = 100$ cm^{-1}. The calculated curve and the experimental data match very well in the temperature range 10−300 K. When $T < 10$ K, the magnetic data are below the calculated curve suggesting that a very small antiferromagnetic interaction between the Co(II) ions occurs. The values of the parameters obtained by the previous fit are within the range of those reported for high spin octahedral Co(II) complexes. For instance, the values of k vary between 0.6 and 0.9 in most six-coordinated Co(II) complexes (so, $k = 0.75$ is found for octahedral Co(II) surrounded by oxygen and nitrogen atoms). The value of λ is slightly smaller than that of the free ion ($\lambda_0 = -180$ cm^{-1}) due to covalency effects. The value of A, about 1.42, is in agreement with the weak ligand field expected for the Co(II) ion in **1**. The value of B/Dq determined by the magnetic susceptibility measurements (1.05) is close to that obtained from electronic spectroscopy (1.08). The corresponding A values differ only in the third digit (1.423 and 1.425), within the range of experimental error. Finally, the absolute value of the energy gap ($|D| = 100$ cm^{-1}) between the orbital singlet $^4A_2$ and the orbital doublet ^4E is small, and this indicates a weak distortion, in agreement with the magnetic moment at room temperature ($D > 0$ means that $^4A_2$ is the ground term). In Figure 3, we plot the theoretical curves for positive and negative D values. The positive D value affords a better fit than the negative D which nevertheless closely follows the experimental data. The sign of D cannot be determined.

The field dependence of the magnetization at 2.0 K, per two Co(II) ions, of a polycrystalline sample of **1** [Figure S3] shows a saturation value M_S of 4.20 $N_A\beta$ at 50 kOe (2.10 $N_A\beta$ per cobalt(II) ion). This value is higher than the calculated M_S value of 3 when $g = 2$. This difference is due to the fact that only the ground Kramers doublet is populated at 2.0 K,[28,29] with an effective spin $S_{eff} = 1/2$ and $g = (10 + 2A\kappa)/3$. For $A = 1.425$ and $k = 0.73$ (see preceding text), $M_S = 2.02$ $N_A\beta$, a value close to the experimental one.

Magnetic susceptibility data of a polycrystalline sample of **2** are shown in Figure 4 under the form of a $\chi_M T$ versus T plot [χ_M is the magnetic susceptibility per Co_3W_2 unit]. At room temperature, $\chi_M T$ is equal to 9.56 cm^3 mol^{-1} K, a value which is expected for two W(V) ($S_W = 1/2$) and three Co(II) magnetically isolated ions ($S_{Co} = 3/2$ with some unquenched orbital moment, as in **1**). On cooling, $\chi_M T$ increases first very smoothly and then rapidly below 20 K up to a maximum around 15 K. Then, it decreases linearly with T as the magnetic susceptibility becomes field dependent.

These observations corresponds to a ferromagnetic interaction between W(V) and Co(II) ions with the onset of a long-range magnetic ordering at low temperatures. The inset of Figure 4 shows the $1/\chi_M$ versus T plot for **2** between 2 and 300 K. Between 50 and 300 K, a Curie−Weiss law fit provides $C = 8.84$ cm^3 mol^{-1} K and $\theta = 23.5$ K. The positive value for θ at high temperature confirms the ferromagnetic interaction between the W(V) and Co(II) ions. To better characterize the ferromagnetic ordering in compound **2**, the temperature dependence of the magnetization at low magnetic field and the remnant magnetization was measured. The field-cooled (FCM), zero-field-cooled (ZFC), and remnant (RM) magnetization curves per Co_3W_2 unit are shown in Figure 5. The FCM curve (30 G applied magnetic field) shows a sharp increase below 22 K and a rapid saturation, demonstrating a long-range order transition. The ZFCM (cooling in zero field and warming under 30 G) merges with the ZFC curve at 18 K (value of the Curie temperature, T_C).

The field dependence of the magnetization per Co_3W_2 unit and the hysteresis loop (inset) at 2 K are shown in Figure 6. The coercive field (H_C) is 600 Oe and the remnant magnetization (M_R) is 4.0$N_A\beta$. The value of M_S is ca. 8.1 $N_A\beta$. Keeping in mind that at 2 K only the ground Kramers doublet of an octahedral Co(II) is populated and that the surroundings of the two different cobalt ions in **2** are similar to the one in **1**, the contribution of the three Co(II) ions to the M_S value in **2** can be estimated as three times that obtained in **1** at 2

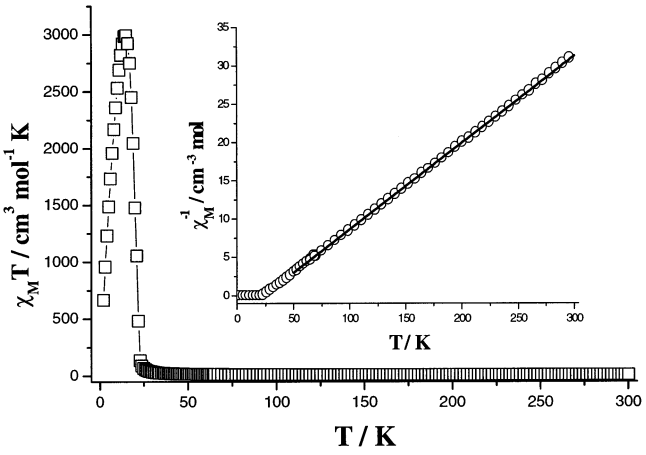

Figure 4. Thermal dependence of the $\chi_M T$ product for compound **2** per Co_3W_2 unit. The inset shows $1/\chi_M$ vs T curve between 2 and 300 K; (—) solid line is the best Curie−Weiss fit between 50 and 300 K.

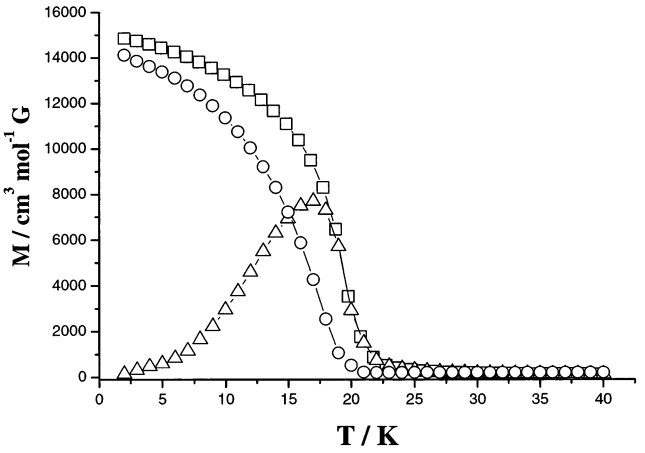

Figure 5. Plots of the magnetization M vs T for a polycrystalline sample of **2** per Co_3W_2 unit: (□) FCM ($H = 30$ Oe), (△) ZFCM ($H = 30$ Oe), and (○) RM.

(28) Carlin, R. L. *Magnetochemistry*; Springer-Verlag: Berlin, 1986.
(29) Coronado, E.; Drillon, M.; Nutgeren, P. R.; De Jongh, L. J.; Beltran, D. *J. Am. Chem. Soc.* **1988**, *110*, 3907.

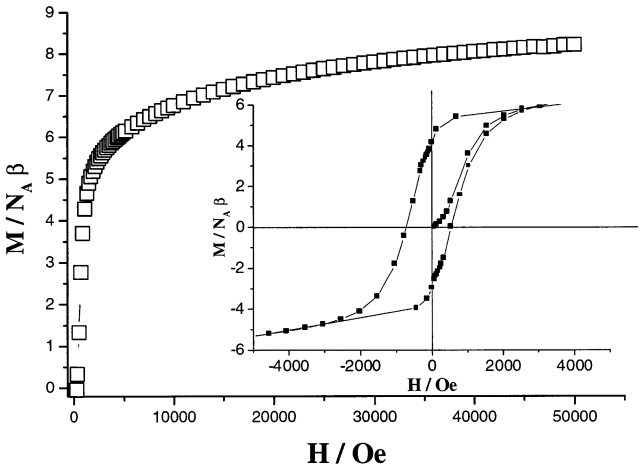

Figure 6. Field dependence of the magnetization M at 2 K of a polycristalline sample of **2** per Co_3W_2 unit. The inset shows the hysteresis loop at 2 K.

K ($3 \times 2.10 = 6.30\ N_A\beta$). The value of the magnetization per W(V) can then be evaluated as $0.9N_A\beta$ corresponding to a g factor of ca. 1.9, as expected for W(V).[30] The same value for g of W(V) is obtained from the Curie constant of **2** ($C = 8.84$ cm^3 mol^{-1} K) and the $\chi_M T$ value of **2** at room temperature.

Finally, the Curie−Weiss constant positive value for **2** ($\theta = +23.5$ K) can be compared to the negative one obtained for the Prussian blue analogue $Co_3[Fe(CN)_6]_2 \cdot 14H_2O$ (Co_3Fe_2) with similar spin carriers ($S_{Fe} = {}^1/_2$) ($\theta = -12$ K).[31] The comparison between the θ values shows that the ferromagnetic (F) interaction in **2** is more important in absolute value than the antiferromagnetic (AF) interaction in Co_3Fe_2. In the frame of Kahn's model of exchange interaction between localized electrons,[32] the coupling constant J is the sum of an antiferromagnetic part J_{AF} and a ferromagnetic one J_F depending on the exchange pathways between the singly occupied orbitals (magnetic orbitals) on each site. In Co_3Fe_2, the Co−NC−Fe unit is linear. The antiferromagnetic term J_{AF} arises from the π overlap of the t_{2g} magnetic orbital on the high spin Co(II) and on the low spin Fe(III). The orthogonality of the two e_g(Co) orbitals (σ-symmetry) with the t_{2g}(Fe) one (π-symmetry) gives rise to a ferromagnetic component J_F that partly counterbalances J_{AF}. Then, the overall coupling constant $J = J_F + J_{AF}$ is antiferromagnetic and weak. In Co_3W_2, the situation is more complex, since there are two cobalt sites, Co(1) and Co(2), and two different $[(NC)_7W-CN-Co(NC)_3(H_2O)_2]$ units and the W−CN−Co(1,2) units are not linear, as shown in Scheme 1A,B.

In both cases, nevertheless, the magnetic orbital of the tungsten is centered on the $5dz^2$ partially delocalized on the π orbitals of the cyanide (Scheme 2C).

The splitting of the d orbital energy of the cobalt, based on simple ligand field considerations, is shown in Scheme 2A (Co(1)) and Scheme 2B (Co(2)), with axes and notations

Scheme 1. Schematic Structure of the W−CN−Co Surroundings in **2** for Co(1) (A) and Co(2) (B)

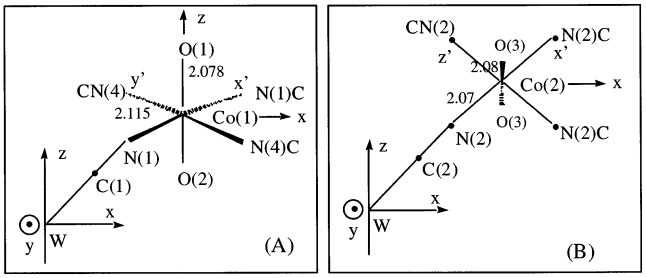

Scheme 2. Schematic Energy Diagrams of Cobalt(II) d-Centered Orbitals (A, B); Schemes of Magnetic Orbitals (C, D) in **2**

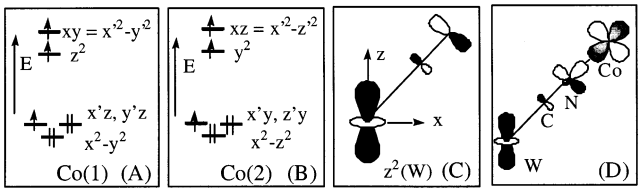

defined in Scheme 1. The three magnetic orbitals of the cobalt(II) [xy, z^2, $y'z$ for Co(1) (Scheme 2A) and xz, y^2, $z'y$ for Co(2) (Scheme 2B)] are orthogonal to the z^2(W), so that the overall interaction J is ferromagnetic. The magnitude of the ferromagnetic coupling is related to the value of the bielectronic exchange integrals k, themselves related to the overlap density ρ between the magnetic orbitals of cobalt and tungsten [ρ = 3d(Co)·5d(W)]. The overlap density ρ is expected to be important on the nitrogen atoms of the cyanide bridge (Scheme 2D) thanks to the delocalization of the diffuse 5d orbitals of tungsten (in black, Schemes 2C,D) and of the magnetic orbitals of cobalt [particularly xy of Co(1) or xz of Co(2) (in gray, Scheme 2D)]. Besides this simple qualitative explanation, our study provides new data to explore more quantitatively the exchange interaction between 3d and 5d metallic ions, computation of the J value, possible role of 5d metal empty orbitals, pointed out recently by Chibotaru et al.,[33] and relativistic effects.

Conclusions

We presented a new example of a three-dimensional molecule-based magnet containing W(V) and Co(II) as magnetic centers, compound **2**, obtained by reaction of octacyanometalate $[W^V(CN)_8]^{3-}$ building blocks with hexaaqua Co(II) ions. Its magnetic properties were analyzed by using as a blank the related paramagnetic three-dimensional compound **1** where the paramagnetic Co(II) ions are bridged by diamagnetic octacyanometalate $[W^{IV}(CN)_8]^{4-}$ units. The ferromagnetism in **2** was qualitatively explained by the orthogonality of the magnetic orbitals on cobalt(II) and tungsten(V). Our results emphasize the importance of unpaired electrons in exchange interaction and related magnetic properties: the Co(II)−W(V) derivative [W(V), $5d^1$, $S = {}^1/_2$] is a magnet whereas the Co(II)−W(IV) derivative [W(IV), $5d^2$, $S = 0$] is a simple paramagnet. An even more striking demonstration is possible with systems presenting the same

(30) Kiernan, P. M.; Griffith, W. P. *J. Chem. Soc., Dalton Trans.* **1975**, 2489.
(31) Gadet, V. Thèse Université P. et M. Curie, Paris, 1992.
(32) Reference 1, p 150sq.
(33) Chibotaru, L. F.; Mironov, V. S.; Ceulemans, A. *Angew. Chem., Int.* Ed. **2001**, *40*, 4423−4433.

stoichiometry, the same structure but different electron counts, to be reported soon.[25]

Acknowledgment. This work was supported by the TMR program from the European Union (Contract ERBFM-RXCT-980181), the Spanish Ministery of Science and Technology (Project BQU2001-2928), and the European Science Foundation through the Molecular Magnets Programme.

Supporting Information Available: Figures S1−S2 (electronic spectrum of **1**), Figure S3 (magnetization vs field) of **1**, Tables S1 and S2 (hydrogen bonds (Å) and bond angles (deg) in compounds **1** and **2**, respectively), and X-ray crystallographic files in CIF format for compounds **1** and **2**. This material is available free of charge via the Internet at http://pubs.acs.org.

IC034188+